RNA (1999), *5*:455–467. Cambridge University Press. Printed in the USA.

Nop58p is a common component of the box C+D snoRNPs that is required for snoRNA stability

DENIS L.J. LAFONTAINE and DAVID TOLLERVEY
Institute of Cell and Molecular Biology, The University of Edinburgh, Edinburgh, Scotland

ABSTRACT

Eukaryotic nucleoli contain a large family of box C+D small nucleolar RNA (snoRNA) species, all of which are associated with a common protein Nop1p/fibrillarin. Nop58p was identified in a screen for synthetic lethality with Nop1p and shown to be an essential nucleolar protein. Here we report that a Protein A-tagged version of Nop58p coprecipitates all tested box C+D snoRNAs and that genetic depletion of Nop58p leads to the loss of all tested box C+D snoRNAs. The box H+ACA class of snoRNAs are not coprecipitated with Nop58p, and are not codepleted. The yeast box C+D snoRNAs include two species, U3 and U14, that are required for the early cleavages in pre-rRNA processing. Consistent with this, Nop58p depletion leads to a strong inhibition of pre-rRNA processing and 18S rRNA synthesis. Unexpectedly, depletion of Nop58p leads to the accumulation of 3′ extended forms of U3 and U24, showing that the protein is also involved in snoRNA synthesis. Nop58p is the second common component of the box C+D snoRNPs to be identified and the first to be shown to be required for the stability and for the synthesis of these snoRNAs.

Keywords: methylation; pre-rRNA processing; ribosome; snoRNA; yeast

INTRODUCTION

Eukaryotic ribosomal RNAs (rRNAs) are synthesized from precursor rRNAs (pre-rRNAs) through a complex processing pathway (Fig. 1; see Eichler & Craig, 1994; Lafontaine & Tollervey, 1995; Venema & Tollervey, 1995; Sollner-Webb et al., 1996; Tollervey, 1996 for recent reviews). While these processing reactions take place, the pre-rRNAs are covalently modified on both the sugar residues (2′-*O*-methylation) and bases (pseudouridine formation and base methylation) (Maden, 1990; Maden & Hughes, 1997) and assemble with the ribosomal proteins into ribonucleoprotein (RNP) particles (Warner, 1989; Raué & Planta, 1991). Most of these steps occur in the nucleolus, a specialized subnuclear compartment (Reeder, 1990; Hernandez-Verdun, 1991; Mélèse & Xue, 1995).

Eukaryotic nucleoli contain a large number of small, metabolically stable RNAs known collectively as the small nucleolar RNAs (snoRNAs) (reviewed in Fournier & Maxwell, 1993; Bachellerie et al., 1995; Maxwell & Fournier, 1995); some 150 snoRNA species are predicted to be present in human cells. Recently, it has become apparent that these snoRNAs fall into two classes that are structurally and functionally distinct (Balakin et al., 1996; Ganot et al., 1997b; Tollervey & Kiss, 1997; reviewed in Lafontaine & Tollervey, 1998). These are designated the box C+D and the box H+ACA snoRNAs after conserved sequence elements that are believed to be sites of RNA–protein interactions. The only exception is the RNA component of the endonuclease RNase MRP, which is related to RNase P (Forster & Altman, 1990; Lygerou et al., 1994; reviewed in Morrissey & Tollervey, 1995).

Within each major family of snoRNAs, two functionally distinct groups can be discerned. A small number of snoRNA species—the box H+ACA snoRNA snR30 and the box C+D snoRNAs U3 and U14—are required for cleavage of the pre-rRNA at the early processing sites, A_0, A_1, and A_2 (Fig. 1; Li et al., 1990; Hughes & Ares, 1991; Morrissey & Tollervey, 1993). Since these cleavages are required for synthesis of the 18S rRNA, this group of snoRNAs are essential for viability. In contrast, the vast majority of snoRNAs function as guide RNAs for the covalent modification of the pre-rRNA and are dispensable for growth. Extended base pairing between a box C+D snoRNA and the rRNA places a predicted protein binding site, box D or D′, at a precise distance of 5 nt from each site of 2′-*O*-methylation (Cavaillé et al., 1996; Kiss-László et al., 1996, 1998; Nicoloso et al., 1996). Similarly, the box H+ACA snoRNAs each form a complex

Reprint requests to: Dr. Denis L.J. Lafontaine, Institute of Cell and Molecular Biology, Swann Building, King's Buildings, The University of Edinburgh, Mayfield Road, EH9 3JR Edinburgh, Scotland; e-mail: denis.lafontaine@ed.ac.uk.

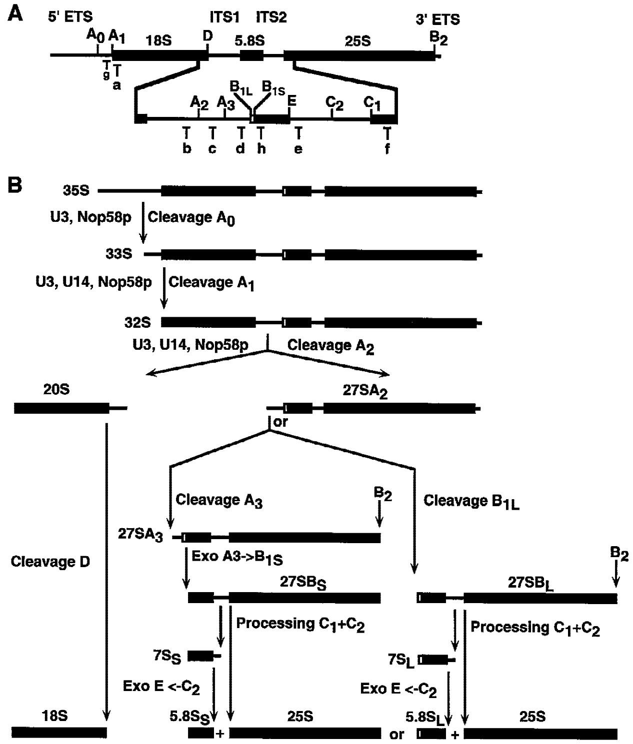

FIGURE 1. Structure of the 35S pre-rRNA and the pre-rRNA processing pathway in *Saccharomyces cerevisiae*. **A**: In the 35S primary transcript, the sequences of the mature 18S, 5.8S, and 25S pre-rRNAs are embedded in the external transcribed spacers (5′ and 3′ ETS) and in the internal transcribed spacers (ITS1 and ITS2). The cleavage sites are indicated by uppercase letters (A_0 to E); the oligonucleotides probes used are indicated by lowercase letters (a to g). **B**: Successive cleavage of the 35S pre-rRNA at sites A_0 and A_1 generates the 33S and 32S pre-rRNAs. Cleavage of the 32S pre-rRNA at site A_2 then generates the 20S and $27SA_2$ pre-rRNAs, which are precursors to the RNA components of the small and large ribosomal subunits, respectively. The mature 18S rRNA is generated by cleavage of the 20S pre-rRNA at site D. The $27SA_2$ precursor is either cleaved at site A_3 by RNase MRP generating the $27SA_3$ pre-rRNA, or at site B_{1L} to yield $27SB_L$ pre-rRNA. The $27SA_3$ pre-rRNA is rapidly digested by the 5′ to 3′ exonucleases Xrn1p and Rat1p to yield the $27SB_S$ pre-rRNA. Processing at site B_2, the 3′ end of the 25S rRNA, is thought to occur while the 5′ ends of the 27SB pre-rRNAs are generated. The $27SB_S$ and $27SB_L$ pre-rRNAs both follow the same pathways of processing to 25S and $5.8S_{S/L}$ through cleavage at sites C_1, the 5′ mature end of the 25S rRNA, and C_2 in ITS2 followed by 3′ to 5′ exonucleolytic digestion of $7S_S$ and $7S_L$ from site C_2 to E by the exosome complex. The early pre-rRNA cleavages at sites A_0, A_1, and A_2 require the box C+D snoRNAs U3 and U14, as well as Nop58p.

pseudoknot structure with the rRNA in which base-paired regions flank a site of pseudouridine (Ψ) formation (Ganot et al., 1997a; Ni et al., 1997). This positions the conserved boxes H or ACA at a fixed distance of ~14 nt from the uracil that is modified by base rotation. In each case this positional information, as well as the overall structure of the snoRNA/pre-rRNA hybrid, is believed to be used by the catalytic activity to select the site of modification. The rRNA 2′-*O*-methyltransferase has not yet been identified but Cbf5p, which is stably associated with the box H+ACA snoRNAs, is likely to be the rRNA Ψ synthase (Koonin, 1996; Henras et al., 1998; Lafontaine et al., 1998a; Watkins et al., 1998a).

The members of each class of snoRNA are associated with common protein components in small nucleolar ribonucleoprotein (snoRNP) particles. Nine proteins common to RNase MRP and RNase P have been identified in yeast (Lygerou et al., 1994; Chu et al., 1997; Dichtl & Tollervey, 1997; Chamberlain et al., 1998), likely representing the complete inventory. Similarly, it is probable that all of the proteins common to the box H+ACA snoRNPs have been found. These are Gar1p (Girard et al., 1992; Balakin et al., 1996; Ganot et al., 1997a), Cbf5p (Lafontaine et al., 1998a), Nhp2p, and Nop10p (Henras et al., 1998; Watkins et al., 1998a). Understanding of the composition of the box C+D class of snoRNPs is less complete, despite the fact that the first component of the box C+D snoRNAs, fibrillarin (Nop1p in yeast), was identified well before any other snoRNP protein (Ochs et al., 1985; Schimmang et al., 1989; Henriquez et al., 1990; Lapeyre et al., 1990; reviewed in Maxwell & Fournier, 1995).

Genetic depletion of Nop1p inhibited cleavage of the pre-rRNA at sites A_0, A_1, and A_2 (Fig. 1) consistent with its association with the U3 and U14 snoRNAs (Schimmang et al., 1989; Tollervey et al., 1991). However, different conditional thermosensitive (ts) alleles of Nop1p had distinct phenotypes, exhibiting defects in either pre-rRNA processing, in pre-rRNA methylation, or in assembly of the ribosomal subunits (Tollervey et al., 1993). The *nop1-3* allele was specifically inhibited for pre-rRNA methylation with little effect on processing, presumably reflecting a general defect in the activities of the methylation guide snoRNAs. *NOP58* was identified in a screen for synthetic lethality with *nop1-3* and Nop58p was shown to be an essential nucleolar protein that copurifies with Nop1p (Gautier et al., 1997). During the course of the present work, Nop58p was independently isolated in a screen for nucleolar antigens and called Nop5p (Wu et al., 1998). Immunoprecipitation with antibodies that recognize Nop5p was reported to coprecipitate four small RNA species that were proposed to be the snoRNAs U3, U14, U18, and snR13 based on their gel mobility (Wu et al., 1998).

The genetic and physical interactions between Nop58p and Nop1p led us to investigate whether Nop58p is itself a common component of the box C+D snoRNPs.

RESULTS

Nop58p is specifically associated with the box C+D snoRNAs

To test whether Nop58p physically interacts with the snoRNAs, we made use of a construct in which the Protein A epitope of *Staphylococcus aureus* is fused in frame with the start codon of Nop58p (Gautier et al., 1997). This construct was expressed in a deleted *nop58*-Δ background and shown to be fully functional (Gautier et al., 1997).

Immunoprecipitation of ProtA-Nop58p with IgG-agarose beads resulted in the coprecipitation of all tested box C+D snoRNAs: U3, U14, U18, U24, snR4, snR13, and snR190 (Fig. 2A, lanes 4–6 and data not shown). The experiment was performed at two salt concentrations: 150 mM KAc (Fig. 2A–C, lanes 4–6) and 500 mM KAc (data not shown). The H+ACA snoRNAs were reported to coprecipitate nonspecifically with Nop1p at 150 mM salt but not in the more stringent conditions of 500 mM KAc (Ganot et al., 1997b). Coprecipitation of the box C+D snoRNAs with Nop58p was observed at both salt concentrations. No precipitation of any RNA was seen with an otherwise isogenic *NOP58* strain expressing only nontagged Nop58p (Fig. 2A-C, lanes 1–3).

Nop58p bears a highly charged, carboxyl KKD/E repeat domain that is also present in other nucleolar proteins (Gautier et al., 1997; Weaver et al., 1997; Lafontaine et al., 1998a). This domain was previously shown to be dispensable both for the nucleolar localization of Nop58p and for its association with Nop1p (Gautier et al., 1997). To test for the potential involvement of the KKD/E repeats in snoRNA association, we used a construct in which a stop codon was introduced by site-directed mutagenesis in the *NOP58* coding region upstream of the KKD/E motif (Gautier et al., 1997). This resulted in the expression of a fusion protein lacking the carboxy-terminal domain. The C+D snoRNAs were recovered with similar efficiency using this construct or the full-length ProtA-fusion protein (Fig. 2A, lanes 7–12). The association of ProtA-Nop58pΔKKD/E with the snoRNAs was unaltered at salt concentrations of 150 mM or 500 mM KAc (Fig. 2A, compare lanes 7–9 with 10–12).

With either ProtA-Nop58p or ProtA-Nop58pΔKKD/E little coprecipitation was observed for the box H+ACA snoRNAs tested: snR3, snR10, snR11, snR30, snR31, snR33, snR36, snR37, or snR42 (Fig. 2B and data not shown). For some species, for example snR3 and snR37, the level of coprecipitation appeared to be above the background in the nontagged strain, but was substantially lower than that of the box C+D snoRNAs. We attribute this to a low level of recovery of higher order nucleolar structures. The MRP RNA was not detectably coprecipitated with Nop58p (Fig. 2C).

We conclude that Nop58p specifically interacts with the box C+D snoRNAs and that this interaction is not dependent on the presence of the charged KKD/E carboxyl domain.

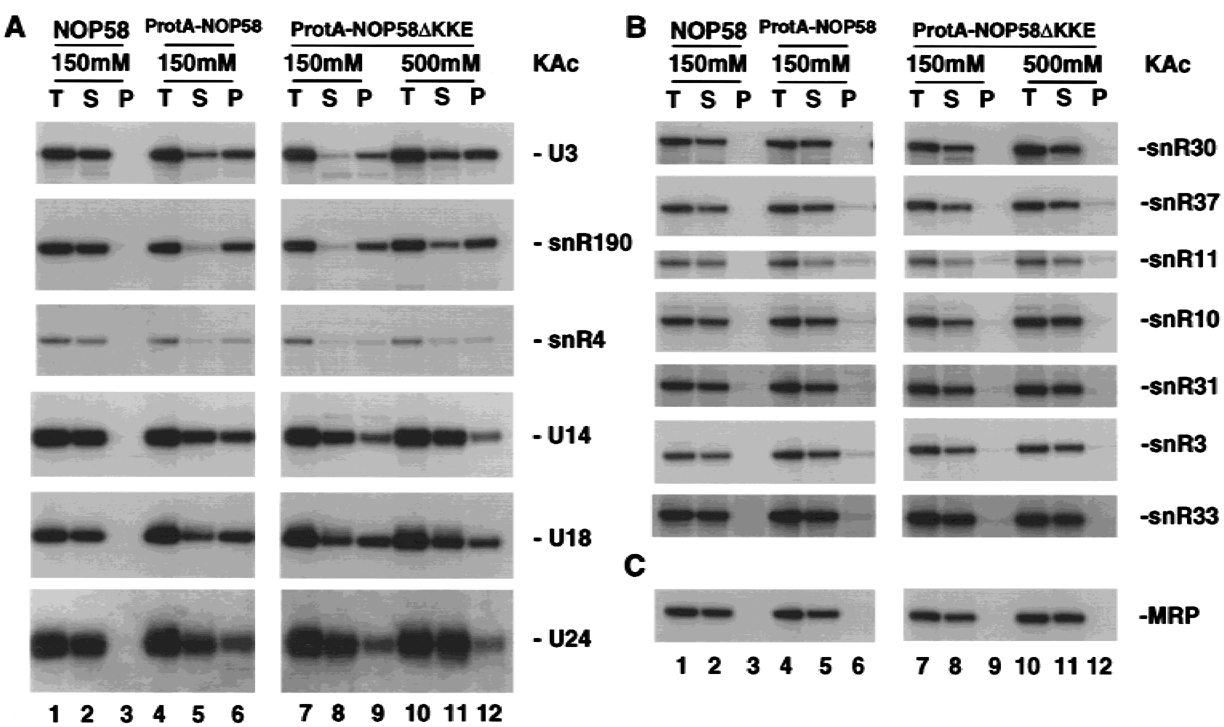

FIGURE 2. Nop58p specifically interacts with the box C+D snoRNAs. Immunoprecipitation on IgG-agarose was performed on lysates from the ProtA-NOP58 and ProtA-NOP58ΔKKE strains and an isogenic wild-type control (NOP58) at the concentrations of KAc indicated. RNA was extracted from equivalent amounts of total (T), supernatant (S), and pellet (P) fractions and separated on a 8% polyacrylamide gel and analyzed by Northern hybridization. **A**: Probes specific for box C+D snoRNAs. **B**: Probes specific for box H+ACA snoRNAs. **C**: probe to the RNase MRP RNA.

Nop58p is required for the stability of the box C+D snoRNAs

To determine whether Nop58p is required for the stability of the box C+D snoRNAs, a conditional mutant was made by replacing the chromosomal *NOP58* promoter region with a repressible *GAL10* promoter (see Fig. 3A and Materials and Methods) using a one-step PCR technique (Lafontaine & Tollervey, 1996). Transcription driven from *GAL* promoters is strongly repressed when strains are grown on glucose medium, allowing the effects of depletion of essential proteins to be followed.

The analyses were performed in duplicate on two independently isolated *GAL::nop58* strains (YDL522-17 and YDL522-20). The data are presented only for strain YDL522-20 as identical results were obtained with the second strain. The *GAL::nop58* strains and the otherwise isogenic wild-type control strain (*NOP58*, strain YDL401) were grown in permissive rsg (raffinose + sucrose + galactose) medium and transferred to glucose-based medium. The growth rate was monitored and total RNA was extracted at various time points after transfer.

Following transfer to glucose medium, the *GAL::nop58* strain is progressively impaired in growth (Fig. 3B). The growth defect follows the depletion of the *NOP58* mRNA (Fig. 3C). In most strains the expression of proteins from genes under *GAL* regulation results in substantial overexpression from the strong *GAL* promoter. This usually contributes to long delays before the onset of the depletion phenotypes (see, e.g., Lafontaine et al., 1995; Dichtl & Tollervey, 1997). In this construct, the structure of the fusion between the *GAL* promoter and *NOP58* gene fortuitously provides a reduced rate of *NOP58* transcription even under permissive conditions (0 h time point) (Fig. 3C, compare lanes 1 and 3). On rsg medium, the growth rate of the *GAL::nop58* strain is reduced by 20% (a doubling time of 150 min for the *GAL::nop58* strain and 120 min for the wild-type).

The steady-state level of various snoRNAs was assessed in the *GAL::nop58* strain by Northern hybrid-

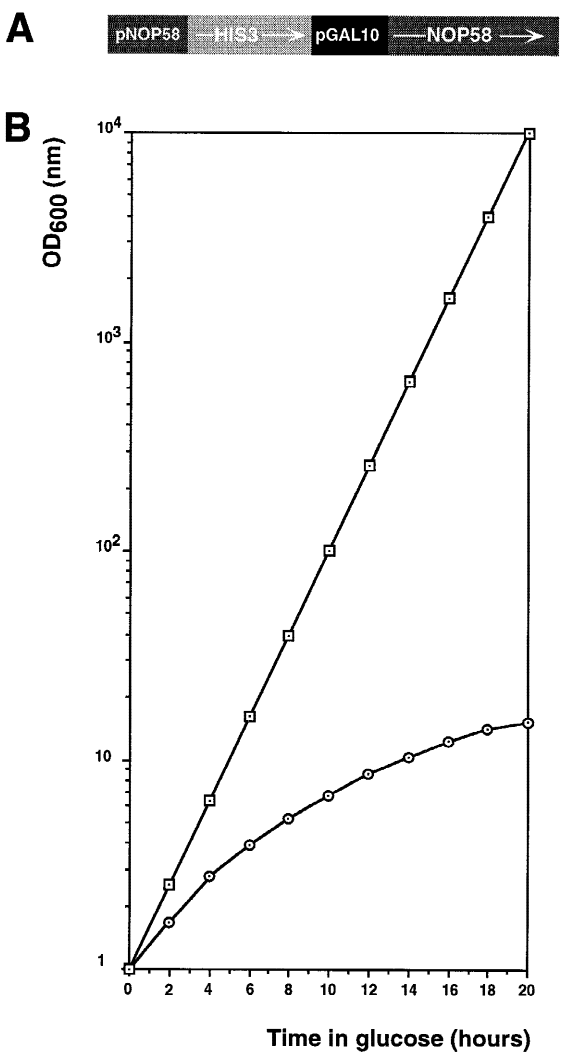

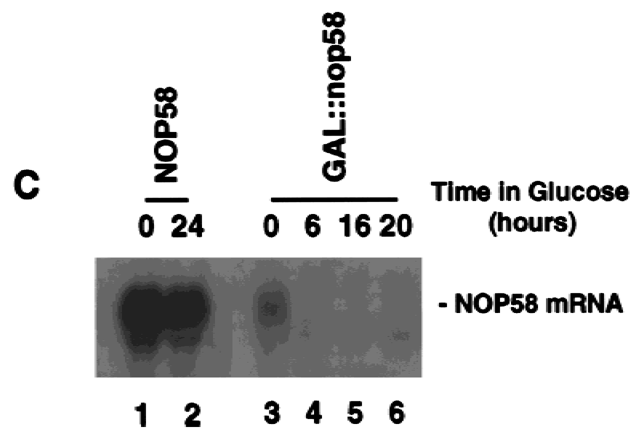

FIGURE 3. Genetic depletion of Nop58p. **A**: Schematic representation of the structure of the *GAL::nop58* allele. **B**: Growth of the *GAL::nop58* (circles) and *NOP58* (squares) strains following transfer to glucose medium. Cell density was measured at regular intervals and the cultures were periodically diluted to be continuously kept in exponential growth. The results are presented on an exponential scale with the OD values corrected for the dilution factor. **C**: Northern hybridization of the *NOP58* mRNA in a *GAL::nop58* strain. RNA was extracted from *NOP58* and *GAL::nop58* strains following growth on permissive rsg medium (0-h lanes) and at intervals following transfer to glucose medium (6–24-h lanes) and separated on a 1.2% agarose gel containing formaldehyde.

ization using specific oligonucleotide probes or antisense RNA transcripts (see Materials and Methods). Strong depletion was observed for all tested box C+D snoRNAs: U3, U14, U18, snR4, snR190 (Fig. 4A), U24 (Fig. 5A,B), and snR13 (data not shown). Consistent with the reduced synthesis of the *NOP58* mRNA under permissive conditions (Fig. 3C), the levels of the C+D snoRNAs are reduced even under permissive conditions (Figs. 4A and 5A,B, lane 3). No depletion was observed for any of the box H+ACA snoRNA tested: snR3, snR10, snR11, snR30, snR31, snR33, snR36, snR37, or snR42 (Fig. 4B and data not shown). The RNase MRP RNA was also unaffected (Fig. 4C).

Among the box C+D snoRNAs tested, some variation in sensitivity to the depletion of Nop58p was observed, with higher residual levels of U3 and U24 than other species. For both of these snoRNAs low levels of longer forms were detected on depletion of Nop58p (Figs. 4A and 5). These extended species were investigated in more detail for U24. Higher resolution Northerns showed that both shorter and longer forms of U24 were accumulated (Fig. 5B). Primer extension from an internal U24 oligonucleotide revealed that the 5′ end of U24 is unaltered in the Nop58p depleted strain (Fig. 5C). RNase protection was used to map the 3′ ends of U24 (Fig. 5D). An antisense transcript overlapping the 3′ end of U24 was annealed to total RNA. The RNA hybrids formed were digested with RNase A + T1 and the protected fragments were resolved on a polyacrylamide gel (see Materials and Methods). The signal detected in the wild-type *NOP58* strain correspond to the position of the authentic 3′ end of U24. In the *GAL::nop58* strain, a protected fragment extended by 5 or 6 nt is detected and accumulates over the time course of depletion (Fig. 5D). This would be in good agreement with the gel mobility of the major extended RNA species seen by Northern hybridization. Why the band corresponding to the size of the mature U24 is not lost from the RNase protection during Nop58p depletion is unclear; we assume this to be an artifact due to the structure of the snoRNA or antisense RNA transcript.

Yeast U24 is encoded in the intron of the *BEL1* gene (Qu et al., 1995) and is produced from the debranched intron-lariat by exonuclease activities (Ooi et al., 1998;

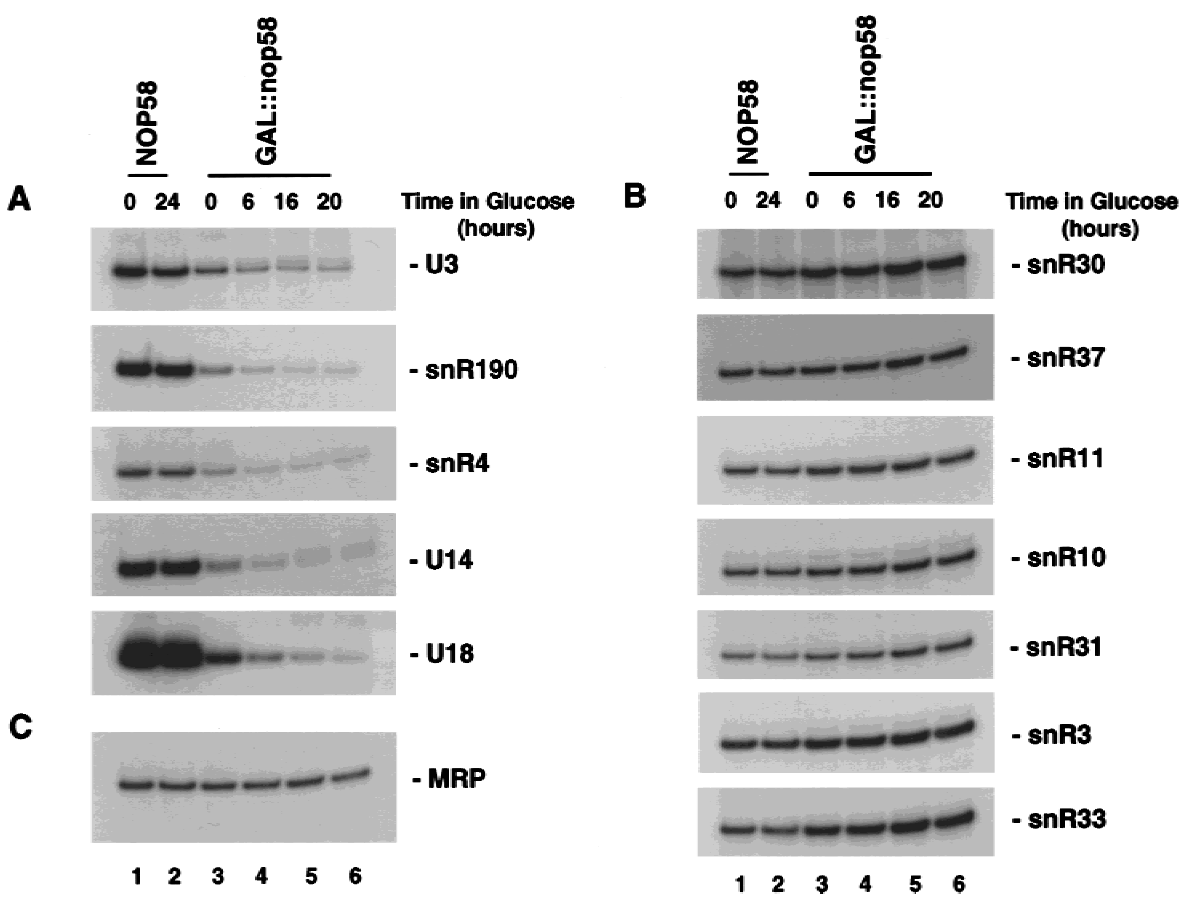

FIGURE 4. The box C+D snoRNAs are specifically depleted in *GAL::nop58* strains. RNA was extracted from *NOP58* and *GAL::nop58* strains following growth on permissive rsg medium (0-h lanes) and at intervals following transfer to glucose medium (6–24-h lanes), separated on a 8% polyacrylamide gel and analyzed by Northern hybridization. **A**: Probes specific for box C+D snoRNAs. **B**: Probes specific for box H+ACA snoRNAs. **C**: Probe to the RNase MRP RNA.

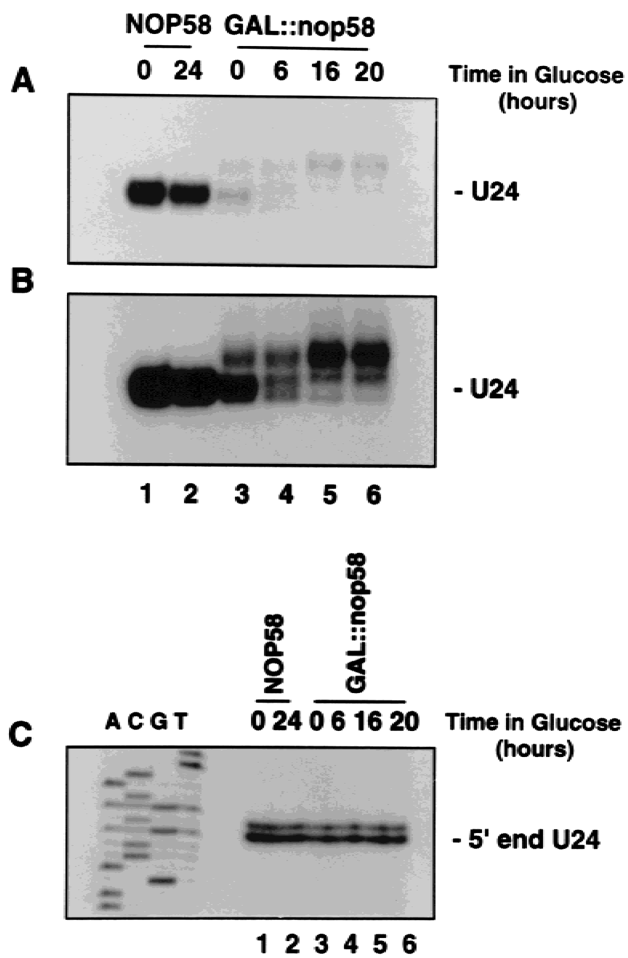

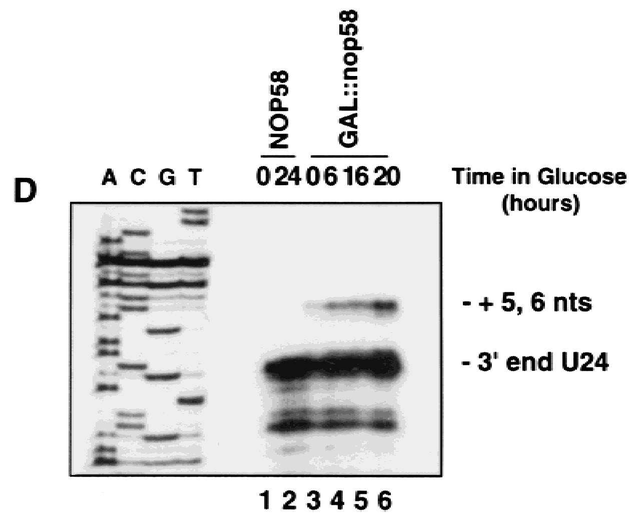

FIGURE 5. 3′ extended forms of the U24 snoRNA accumulate in *GAL::nop58* strains. **A**: Northern analysis of the steady-state levels of U24. **B**: Longer exposure of the hybridization shown in **A**. **C**: Primer extension mapping of U24 5′ ends. **D**: RNase A/T1 mapping of U24 3′ ends. RNA was extracted from *NOP58* and *GAL::nop58* strains following growth on permissive rsg medium (0-h lanes) and at intervals following transfer to glucose medium (6–24-h lanes) and either separated on a 8% polyacrylamide gel and analyzed by Northern hybridization or processed for primer extension or RNase A/T1 analysis.

Petfalski et al., 1998). We conclude that depletion of Nop58p interferes with normal 3′ processing of U24.

The stability of Nop1p/fibrillarin, the other major box C+D snoRNP protein component, was also tested on Nop58p depletion (Fig. 6). Equivalent amounts of total protein extracted from cells depleted for various time points of transfer in nonpermissive conditions were used in an immunoblot experiment with anti-Nop1p antibody. This analysis revealed that the steady-state level of Nop1p is not affected by the depletion of Nop58p. We conclude that Nop58p is specifically required for the stability of the box C+D snoRNAs and that Nop1p is stable in the absence of snoRNA association.

Nop58p is required for 18S rRNA synthesis

Depletion of U3 and U14 snoRNAs in the *GAL::nop58* strain was predicted to inhibit pre-rRNA processing. This was therefore analyzed by Northern hybridization (Fig. 7) and primer extension (Fig. 8) using a set of oligonucleotide probes specific for the pre-rRNA species and mature rRNAs (see Fig. 1A for the locations of the probes used).

In wild-type strains, the 35S pre-rRNA is cleaved sequentially at sites A_0, A_1, and A_2 (see Fig. 1B); these processing reactions require the box C+D snoRNAs U3 and U14 (Li et al., 1990; Hughes & Ares, 1991). Cleavage at A_0 produces the 33S pre-rRNA (which cannot be detected in wild-type strains by Northern hybrid-

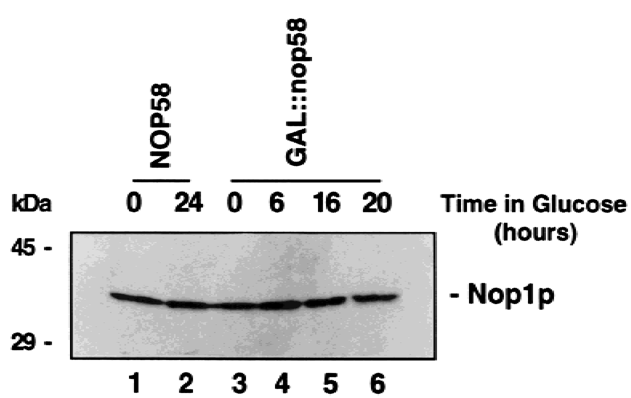

FIGURE 6. Steady-state level of Nop1p/fibrillarin on Nop58p depletion. Proteins were extracted from *NOP58* and *GAL::nop58* strains following growth on permissive rsg medium (0-h lanes) and at intervals following transfer to glucose medium (6–24-h lanes), separated on 15% SDS-PAGE gel and analyzed by Western-blotting with anti-Nop1p antibody. Nop1p (Mr 34.5 kDa) migrates with an apparent size of 38 kDa (Schimmang et al., 1989).

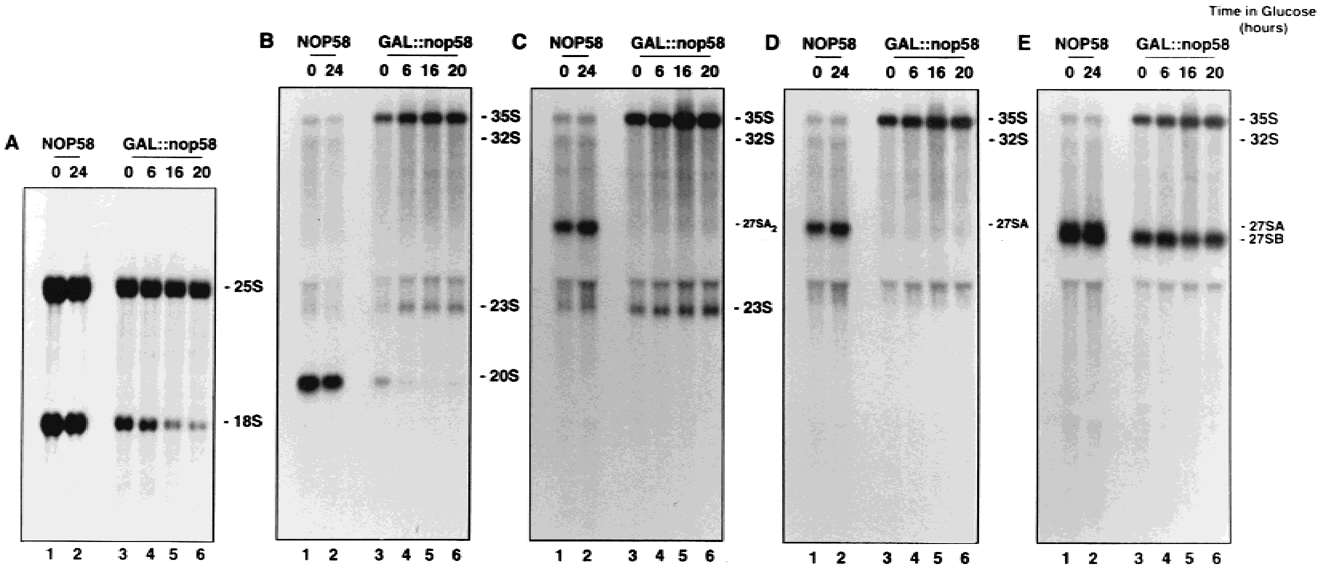

FIGURE 7. Northern analysis of rRNA and pre-rRNA synthesis in a *GAL::nop58* strain. **A**: Probes against mature 25S and 18S rRNA (oligonucleotides a and f). **B**: Probe against the 5′ region of ITS1 (oligonucleotide b). **C**: Probe against ITS1 between sites A_2 and A_3 (oligonucleotide c). **D**: Probe against the 3′ region of ITS1 (oligonucleotide d). **E**: Probe against the 5′ region of ITS2 (oligonucleotide e). The oligonucleotides used are depicted in Figure 1A. Oligos d and e do not distinguish between 27SA$_2$ and 27SA$_3$. RNA was extracted from *NOP58* and *GAL::nop58* strains following growth on permissive rsg medium (0-h lanes) and at intervals following transfer to glucose medium (6–24-h lanes), separated on a 1.2% agarose gel containing formaldehyde and analyzed by Northern hybridization.

ization), A_1 cleavage generates the 32S pre-rRNA, and A_2 cleavage produces the 20S and 27SA$_2$ pre-rRNAs. The 20S pre-rRNA is processed to mature 18S rRNA, whereas the 27SA$_2$ pre-rRNA is processed to mature 5.8S and 25S rRNA. In the *GAL::nop58* strain, these three early cleavages were inhibited. Consequently, the 35S pre-rRNA (Fig. 7B–E) was accumulated, whereas synthesis of the 32S (Fig. 7B–E), 20S (Fig. 7B), and 27SA$_2$ pre-rRNAs (Fig. 7C) was inhibited. Instead, the 35S pre-rRNA was predominantly cleaved at site A_3 by RNase MRP. This cleavage generates an abnormal species, the 23S RNA (Fig. 7B,C), and the 27SA$_3$ pre-rRNA, which is not readily detected by Northern hybridization. The 23S pre-rRNA extends from the 5′ end of the 35S pre-rRNA to site A_3 and was detected with probes g, b, and c (Fig. 7B,C and data not shown), but not with probes specific to sequences 3′ to site A_3 (oligos d and e, Fig. 7D,E). The 23S pre-rRNA is rapidly degraded and synthesis of 18S rRNA is therefore predicted to be inhibited, leading to the observed depletion (Fig. 7A). The levels of the 27SB pre-rRNA (Fig. 7E) and the mature 25S rRNA (Fig. 7A) and 5.8S rRNA (data not shown) were not affected by depletion of Nop58p, indicating that subsequent processing of the 27SA$_3$ pre-rRNA is normal. Consistent with the levels of the snoRNAs (Figs. 4A and 5A,B), pre-rRNA processing in the *GAL::nop58* strain is partially inhibited under permissive conditions (0 h samples), and is progressively more inhibited after transfer to glucose medium (6–20 h samples).

In agreement with the Northern data, primer extension through the 5′ ETS from primer a (complementary to the 5′ end of 18S rRNA) showed an increase in the stop at position +1, the 5′ end of the 35S pre-rRNA (Fig. 8). In contrast, the level of the stop at site A_0, the 5′ end of the 33S pre-rRNA was reduced.

Primer extension through ITS1 from primer e (complementary to a sequence in the 5′ region of ITS2) confirmed the strong inhibition of cleavage at site A_2 (Fig. 8). In contrast, the stop at site A_3, the 5′ end of 27SA$_3$, was not affected in the *GAL::nop58* strain. The stop at site B_{1S}, the 5′ end of the 27SB$_S$ and 7S$_S$ pre-rRNAs, was also unaffected (Fig. 8), indicating that subsequent processing of the 27SA$_3$ pre-rRNA is not inhibited by Nop58p depletion. The alternative pre-rRNA processing pathway through processing at site B_{1L} (see legend to Fig. 1B) was also unaffected by Nop58p depletion as shown by the stop at site B_{1L}, the 5′ end of the 27SB$_L$, and 7S$_L$ pre-rRNAs (Fig. 8) and by the unaltered ratio of mature 5.8S$_L$:5.8S$_S$ (data not shown) in the *GAL::nop58* strain.

We conclude that Nop58p is specifically required for pre-rRNA cleavage at sites A_0, A_1, and A_2. The inhibition of processing is most likely a consequence of the reduced levels of the U3 and U14 snoRNAs. As judged by primer extension, depletion of U3 leads to a strong reduction in the steady-state level of the 33S pre-rRNA, whereas depletion of U14 does not (Hughes & Ares, 1991; Beltrame et al., 1994). The loss of the 33S pre-rRNA is, therefore, likely to be a specific conse-

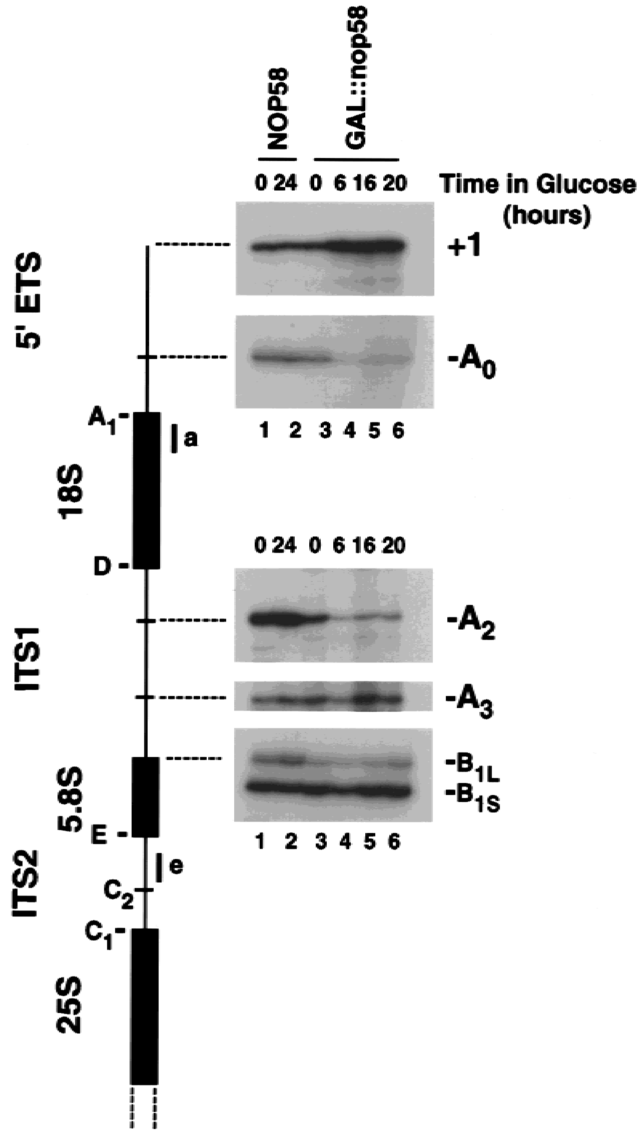

FIGURE 8. Primer extension analysis of pre-rRNA processing in a *GAL::nop58* strain. Primer extension through the 5′ ETS and ITS1 was performed using oligonucleotides a and e, respectively (see cartoon). Primer extension stops at the 5′ end of the 5′ ETS (+1) and at sites A_0, A_2, A_3, B_{1L}, and B_{1S} are indicated. RNA was extracted from *NOP58* and *GAL::nop58* strains following growth on permissive rsg medium (0-h lanes) and at intervals following transfer to glucose medium (6–24-h lanes).

quence of the depletion of U3 in the *GAL::nop58* mutant. Interestingly, the level of 33S pre-rRNA is not clearly reduced in the 0 h samples, whereas the levels of 32S, 20S, and 27SA$_2$ are strongly reduced. This may be related to the greater reduction in the level of U14 than U3 at this time point (Fig. 4A).

The effects of depletion of Nop58p on 2′-*O*-methylation were assessed by metabolic labeling. A *GAL::nop58* strain and the otherwise isogenic wild-type control (*NOP58*) were grown in minimal rsg medium and transferred to glucose for 6 h before being pulse-labeled for 5 min with either [^{3}H]-methionine or [^{3}H]-uracil. Total RNA was extracted from the same numbers of cells, separated on 1.2% agarose/formaldehyde gels, transferred to Genescreen membranes and visualized by fluorography. Consistent with the results of Northern hybridization, the 35S pre-rRNA was accumulated while the 27SA and 20S pre-rRNAs were underaccumulated in the Nop58p depleted strain. Synthesis of the 18S rRNA was inhibited compared to 25S rRNA (data not shown). In duplicate experiments, identical areas of membranes corresponding to the positions of the mature 18S and 25S rRNAs were excised and submitted to liquid scintillation counting. Surprisingly, in three independent experiments the incorporation of tritiated methionine into the rRNAs in the Nop58p depleted strain was not substantially decreased as compared to the incorporation of tritiated uracil (data not shown). Incorporation of both isotopes was, however, greatly reduced in the Nop58p-depleted strain, presumably because of its slow growth rate. We conclude that methylation of the pre-rRNA is substantially more resistant to reduced snoRNA levels than is pre-rRNA cleavage.

DISCUSSION

We report here that the essential nucleolar protein Nop58p is specifically associated with one of the two major classes of snoRNAs, the box C+D snoRNAs. Immunoprecipitation using Nop58p epitope-tagged with Protein A efficiently precipitated all tested box C+D snoRNAs. The association of Nop58p with the box C+D snoRNAs was found to be specific, since neither the box H+ACA snoRNAs nor the RNase MRP RNA were significantly coprecipitated. In addition, Nop58p was shown to be required for the stability of the box C+D snoRNAs; genetic depletion of Nop58p leads to the dramatic depletion of most box C+D snoRNAs tested. This effect was specific because neither the H+ACA snoRNAs nor the RNase MRP RNA were affected. We conclude that Nop58p is a core component of the box C+D snoRNPs, and is the first protein shown to be required for the stability of these RNA species. UV cross-linking of box C+D RNA reporter constructs in mouse nuclear extracts and *Xenopus* oocytes identified putative snoRNP proteins that require intact boxes C and D and the conserved 5′-3′ terminal stem for binding. Among these were fibrillarin and a protein of 65–68 kD apparent molecular weight (Caffarelli et al., 1998; Watkins et al., 1998b), in good agreement with the predicted size of human Nop58p (Wu et al., 1998).

Searches of the complete genomic sequences of the Archaea *Archaeoglobus fulgidus* (Klenk et al., 1997), *Methanobacterium thermoautotrophicum* (Smith et al., 1997), and *Methanococcus jannaschii* (Bult et al., 1996) identified predicted proteins in each organism with clear homology to Nop58p. Comparison to the yeast/human alignments indicate that the archaeal proteins are rather more homologous to Nop58p than to Nop56p. Homologs of the other common protein component of the box C+D snoRNPs, Nop1p/fibrillarin, have previously been identified in Archaea (Amiri, 1994) and are also present in the complete genomic sequences. Strikingly, the genes encoding the homologs of Nop58p and Nop1p appear to be cotranscribed as an operon in both *A. fulgidus* and *M. thermoautotrophicum*, strongly supporting their functional conservation. In *M. jannaschii* the genes are closely located in the genome but do not appear to form an operon. The presence and genomic organization of the homologs of both known box C+D snoRNP proteins suggests that homologs of the box C+D snoRNAs may also be present in Archaea (see Lafontaine & Tollervey, 1998 for further discussion).

There are similarities between the proteins associated with the box C+D and box H+ACA snoRNAs. Both groups are associated with a protein that contains a glycine/arginine rich repeat (GAR domain or RGG box); the box C+D snoRNAs are associated with Nop1p, and the box H+ACA snoRNAs with Gar1p. Similarly, both groups are associated with proteins containing a KKD/E domain; Cbf5p (dyskerin in humans; Heiss et al., 1998) is associated with the box H+ACA snoRNAs and Nop58p with the box C+D snoRNAs. However, whereas the H+ACA snoRNP proteins Cbf5p, Nhp2p, and Nop10p are each required for the stability of Gar1p (Henras et al., 1998; Lafontaine et al., 1998a), Nop58p is not required for the stability of Nop1p.

The bulk of the box C+D snoRNAs are predicted to act as guides to select sites of 2′-*O*-methylation in the pre-rRNA. However, two box C+D species, U3 and U14, are required for pre-rRNA processing. Genetic depletion of U3 inhibits pre-rRNA cleavage at sites A_0, A_1, and A_2; depletion of U14 strongly inhibits cleavage at A_1 and A_2, but has less effect on processing at site A_0 (Fig. 1B; Li et al., 1990; Hughes & Ares, 1991; Beltrame et al., 1994). These three early cleavages are all greatly inhibited in the Nop58p depleted strain (see also Wu et al., 1998). This leads to a strong impairment in the synthesis of the 18S rRNA, preventing synthesis of the small ribosomal subunits. This inhibition most likely underlies the lethality seen on deletion of the *NOP58* gene (Gautier et al., 1997) or on genetic depletion of Nop58p.

Incorporation of [^{3}H]-uracil into newly synthesized pre-rRNA was strongly reduced (approximately fivefold after 6 h in minimal glucose medium), presumably because of the slowed growth rate of the Nop58p depleted cells. Surprisingly, the incorporation of [^{3}H]-methionine into methyl groups in the pre-rRNA was reduced to the same extent. The reduced level of pre-rRNA detected by uracil labeling is unlikely to be due to destabilization of under-methylated pre-rRNA; in strains carrying the ts-lethal *nop1-3* mutation, methylation of the pre-rRNA was very strongly inhibited with little effect on pre-rRNA or rRNA synthesis (Tollervey et al., 1993). The residual levels of the box C+D snoRNAs present in the Nop58p depleted strain appear to be sufficient to direct the efficient methylation of the low residual levels of pre-rRNA, although it may be that a few specific sites of 2′-*O*-methylation are more severely inhibited than is indicated by the data on bulk methylation. In contrast, cleavage of the pre-rRNA at sites $A_0/A_1/A_2$ was strongly inhibited under the same conditions. This indicates that higher levels of U3 and/or U14 are required to support pre-rRNA cleavage than are generally required for activity of the methylation guides. It is notable that strains depleted of Nop1p/fibrillarin are strongly inhibited for pre-rRNA processing but have only a mild methylation defect, even though the *nop1-3* allele shows strong inhibition of methylation (Tollervey et al., 1991, 1993). One explanation would be that the pre-rRNA/snoRNA association must be sustained for longer periods of time to direct the cleavage reactions. Binding of U14 to the pre-rRNA in the 18S rRNA region and binding of U3 to the 5′ ETS region are required for the early pre-rRNA cleavages (Beltrame & Tollervey, 1992, 1995; Liang & Fournier, 1995) and the time taken for these three cleavages to occur may become limiting under conditions of snoRNA depletion. Moreover, there is likely to be a limited time window for the cleavage of sites $A_0/A_1/A_2$. If the pre-rRNA is cleaved at site A_3 by RNase MRP, the resulting 23S RNA is very rapidly degraded by the exosome complex of 3′ → 5′ exonucleases (P. Mitchell, E. Petfalski, D. Tollervey, unpubl.) preventing synthesis of the 18S rRNA.

Comparison of different box C+D snoRNAs revealed some variation in the residual levels on depletion of Nop58p. For U3, a longer species accumulated, clearly showing an effect on synthesis of the snoRNA. The 5′ end of mature U3 corresponds to the tri-methyl guanosine cap of the primary transcript, and the extended form is therefore very likely to be 3′ extended. In vertebrates and yeast, spliceosomal snRNAs are processed from precursors with 3′ extensions (Madore et al., 1984a, 1984b; Yuo et al., 1985; Chanfreau et al., 1997; Abou Elela & Ares, 1998), and U3 may be similarly processed. Longer forms of U24 were also accumulated, together with low levels of shorter forms. The 5′ end of U24 was unaffected by depletion of Nop58p whereas RNase protection experiments detected species 3′ extended by 5–6 nt, showing these changes to be due to alterations in 3′ processing. Yeast U24 is encoded in the intron of the *BEL1* gene (Qu et al., 1995) and the snoRNA is obligatorily synthesized from the intron following debranching of the intron lariat; very low levels of mature U24 are synthesized in a *dbr1*-Δ strain that lacks debranching activity (Ooi et al., 1998; Petfalski et al., 1998). This strongly indicates that both ends of U24 are synthesized by exonucleolytic activities and, indeed, the 5′ → 3′ exonucleases Rat1p and Xrn1p were identified as the activities responsible for the 5′ processing (Petfalski et al., 1998). In vertebrates, the 5′ and 3′ ends of all tested intron-encoded snoRNAs are synthesized by exonucleases

(Cecconi et al., 1995; Kiss & Filipowicz, 1995; Caffarelli et al., 1996; Cavaillé & Bachellerie, 1996; Kiss et al., 1996; Xia et al., 1997).

The box C+D sequences, together with a stem structure that normally brings them together in the snoRNA secondary structure are the only elements essential for the synthesis and stability of this class of snoRNA, and their presence is the only feature that is clearly conserved among the box C+D snoRNAs (Baserga et al., 1991; Huang et al., 1992; Caffarelli et al., 1996; Watkins et al., 1996; Xia et al., 1997). A simple model for the involvement of Nop58p in snoRNA stability is through protection from the exonucleolytic activities that normally generate the mature ends. If so, the alteration in the 3′ end of U24 on depletion of Nop58p suggests that this interaction might be via binding to the conserved box D at the 3′ end of the snoRNAs. Curiously, inspection of the 3′ end of U24 (**CUGA**UGAAU$_{OH}$) (Qu et al., 1995) reveals the presence of a consensus box C motif (UGAUGA), partially overlapping the box D element (**CUGA**). We speculate that on depletion of Nop58p, the putative box C binding protein(s), which normally binds to the 5′ end of the snoRNA, also binds to the cryptic 3′ box C element. This might confer extra protection to U24 and explain why this species is more resistant to Nop58p depletion.

During depletion of Nop58p, Nop1p was reported to be delocalized to the nucleoplasm and cytoplasm (Wu et al., 1998). In the conditions used (up to 12 h in glucose medium) the snoRNAs were presumably strongly depleted. This indicates that Nop1p does not localize to the nucleolus on its own, but rather is localized to and/or anchored to the nucleolus in association with snoRNPs. The association of the box C+D snoRNAs with the nucleolus does not require complementarity to the pre-rRNA (Lange et al., 1998b). Instead, both snoRNA stability and nucleolar targeting require the conserved box C+D elements and the terminal stem (Lange et al., 1998a, 1998c; Samarsky et al., 1998). It seems probable that Nop58p stabilizes the snoRNAs via binding to one or both of these sequence elements and is, therefore, a good candidate to provide the nucleolar targeting signals. Testing of this hypothesis will require the separation of the role of Nop58p in snoRNA stability from its putative targeting function.

MATERIALS AND METHODS

Construction of Nop58p epitope tagged and *GAL::nop58* strains

Strains used for the immunoprecipitation experiments, ProtA-NOP58, ProtA-NOP58ΔKKE, and the wild-type isogenic control (NOP58) were generously provided by T. Gautier (Université I, Grenoble) and were described previously (Gautier et al., 1997). In these haploid strains, a chromosomal *nop58Δ::HIS3* deletion is rescued either by plasmids, pRS315-ProtA-NOP58, pRS315-ProtA-NOP58ΔKKE, or pRS315-NOP58. Both ProtA-NOP58 and ProtA-NOP58-ΔKKE epitope-tagged fusions of Nop58p were showed to be fully functional. The control ProtA-NOP1 strain was a generous gift from E. Hurt.

The *GAL::nop58* strain was constructed in strain YDL401 (Lafontaine & Tollervey, 1996) by use of a one-step PCR strategy (Lafontaine & Tollervey, 1996). This resulted in the direct fusion on the chromosome of a *HIS3-pGAL* cassette in front of the ATG of *NOP58*. The oligonucleotides used for the amplification with plasmid pTL26 were oligonucleotide 1, 5′-TGCTTTCGCAAAAATTTCGCATATAAGTTATTTTTGAAATA GCAGCTCTTGGCCTCCTCTAGT-3′ and oligonucleotide 2, 5′-ACCAGCTGAAGTTTCAGTTAAAACGTAAGCCATTGT ATGAGGAGGTTGCGAATTCCTTGAATTTTCAAA-3′. Transformants were screened for glucose sensitivity and by PCR on yeast colonies. RNA analyses presented in Figures 3, 4, and 7 were performed in duplicate on two independently isolated *GAL::nop58* strains (YDL522-17 and YDL522-20); analysis presented in Figures 5 and 8 were made on strain YDL522-20.

Immunoprecipitation of ProtA-Nop58p and ProtA-Nop58pΔKKE

Immunoprecipitation experiments were performed essentially as described in Lafontaine et al. (1998a). Yeast whole-cell extracts were prepared as described in Séraphin & Rosbash (1989). Lysates were made in buffer A (20 mM Tris HCl, pH 8.0, 5 mM $MgCl_2$, 1 mM DTT, 0.2% Triton X-100, 0.5 mM PMSF, and 150 mM or 500 mM K acetate), and supernatants were cleared by centrifugation (56,000 rpm, 4 °C, 20 min). Lysates equivalent to 37.5 OD_{600} of cells were incubated on a rotating wheel for 2 h at 4 °C with 100 μL of IgG-agarose beads (Sigma, A2909), prewashed in buffer A, in a total volume of 400 μL. Pellets were washed four times for 20 min in 1 mL of buffer A. Each gel lane (T, S, P) was loaded with RNA from a fraction of the preparation equivalent to 10 OD_{600} of cells.

GAL::nop58 time course, RNA extraction, Northern-blot hybridization and primer extension

For depletion of Nop58p, cells growing exponentially in permissive rsg conditions (2% galactose, 2% sucrose, and 2% raffinose complete medium) at 30 °C were harvested by centrifugation, washed, and resuspended in prewarmed YPD (2% glucose complete medium). During growth, cells were diluted with prewarmed medium and constantly maintained in exponential phase. RNA extraction, Northern hybridization, and primer extension were as described in Lafontaine et al. (1995, 1998b). Standard 1.2% agarose/formaldehyde and 8% acrylamide gels were used to analyze the processing of the high- and low-molecular weight rRNAs species, respectively. Nine micrograms of total RNA were used for the Northern and primer-extension experiments presented in Figures 3–5, 7, and 8.

Oligonucleotides used for pre-rRNA hybridization were: oligo a = CATGGCTTAATCTTTGAGAC, b = CGGTTTTAATTGT CCTA, c = TTGTTACCTCTGGGCCC, d = CCAGTTAC GAAAATTCTTG, e = GGCCAGCAATTTCAAGTTA, f = CTCCGCTTATTGATATGC, g = CCAGATAACTATCTTAA AAG, and h = TTTCGCTGCGTTCTTCATC.

Oligonucleotides used for snoRNA hybridization were: oligo anti-U3 = UUAUGGGACUUGUU, snR190 = CGTCATGGT CGAATCGG, snR4 = CACAATCCACATCGACCC, U14 = TCACTCAGACATCCTAGG, U18 = GTCAGATACTGTGAT AGTC, U24 = TCAGAGATCTTGGTGATAAT, snR13 = CA CCGTTACTGATTTGGC, snR37 = GATAGTATTAACCAC TACTG, snR11 = GACGAATCGTGACTCTG, snR31 = GT AGAACGAATCATGACC, snR3 = TCGATCTTCGTACTGTCT, snR33 = GATTGTCCACACACTTCT, snR36 = CATCCAGC TCAAGATCG, snR42 = CTCCCTAAAGCATCACAA, and MRP = AATAGAGGTACCAGGTCAAGAAGC. Antisense transcripts specific to snR30 and snR10 were made from vectors pT3/T7-snR30 (Morrissey & Tollervey, 1993) and pT3/T7-snR10 following appropriate linearization. To detect the *NOP58* mRNA, a fragment spanning the whole ORF of *NOP58* was generated by PCR and labeled using the Prime-a-Gene Labeling kit (Promega).

Western blotting analysis

For protein extraction, cells equivalent to 10 OD_{600} were harvested and resuspended in 200 μL of SDS loading buffer with 50 μL of glass beads. Cells were vortexed for 1 min and incubated for 1 min at 95 °C three times successively. Lysates were cleared by centrifugation for 10 min at 14,000 rpm and supernatants equivalent to 0.375 OD_{600} units of cell were loaded per lane. Samples were run on a 15% SDS-PAGE gel and blotted according to standard procedures. The blot was decorated with monoclonal mouse anti-Nop1p antibody (mA66, dilution 1/20, kindly provided by J. Aris) and developed using the ECL detection kit (Amersham).

RNase A/T1 mapping

RNase A/T1 protection analysis was essentially performed as described in Goodall et al. (1990). The ^{32}P-labeled antisense probe was transcribed with T7 polymerase from plasmid pTL66 linearized with *Eco*57 I. The probe was treated with RQ1-RNase-free DNase (Promega) and gel purified. Nine micrograms of total RNA were mixed with ~40 cpm of probe in 30 μL of PIPES buffer (40 mM PIPES, pH 6.7, 400 mM NaCl, 1 mM EDTA)/50% formamide. Annealing was performed overnight at 48 °C. Digestion in RNase buffer (10 mM Tris HCl, pH 7.5, 300 mM NaCl, 1 mM EDTA) was with 7.5 U of RNase T1/1.5 μg RNase A (both purchased from Boehringer) for 30 min at 25 °C. Protected products were recovered by phenol-chloroform extraction and separated on an 8% polyacrylamide gel. A sequencing reaction was used as a ladder. With the antisense U24 transcript used (212 nt), the protected fragment corresponding to the mature 3′ end of U24 was detected at the expected length of 77 nt. Plasmid pTL66 was constructed as follows: a U24 genomic fragment encompassing the 3′ end of U24 was recovered by *Kpn*I/*Dra*I digestion from plasmid pFH2 (a kind gift of Y. Henry) and subcloned in pBluescript.

Analysis of methylation levels

The overall level of rRNA methylation was assessed by in vivo pulse labeling of the RNAs with either [^{3}H]-uracil or [^{3}H]-methionine followed by autoradiography and liquid scintillation counting. A *GAL::nop58* strain (YDL522-20) and the isogenic wild-type control (YDL401), transformed with a plasmid expressing the *URA3* gene (pFL44S) (Bonneaud et al., 1991), were grown at 30 °C in minimal medium lacking uracil, methionine, and histidine and containing 2% galactose, 2% sucrose, and 2% raffinose. Exponentially growing cells were washed and transferred to prewarmed minimal medium lacking uracil, methionine, and histidine and containing 2% glucose. At the identical OD_{600} of 0.35 (for the *GAL::nop58* strain, this corresponded to a transfer of 6 h in nonpermissive conditions), wild-type and mutant cells were pulse-labeled for 5 min with 100 μCi/mL of either [^{3}H]-uracil or [^{3}H]-methionine. One milliliter aliquots of cultures were snap-frozen in liquid nitrogen. Total RNA was extracted and resolved on a 1.2% agarose/formaldehyde gel. Gels were transferred to Genescreen plus membranes (NEF-976, Dupont De Nemours), sprayed with tritium enhancer (NEF-970G, Dupont De Nemours), and exposed for autoradiography. In duplicate experiments, identical areas of membranes corresponding to the mature 18S and 25S rRNA (as judged by Ethidium bromide staining) were cut and submitted to liquid scintillation counting using the Ultima-Gold F scintillant (Packard Bioscience).

ACKNOWLEDGMENTS

We would like to thank Ed Hurt (Universität Heidelberg) for supplying the ProtA-Nop1p construct, Y. Henry (CNRS, Toulouse) for plasmid pFH2, and, particularly, Thierry Gautier (Université I, Grenoble) and Ed Hurt for the ProtA-Nop58p constructs. DLJL was the recipient of a fellowship from the European Union TMR programme. This work was supported by the Wellcome Trust.

Received October 14, 1998; returned for revision November 13, 1998; revised manuscript received December 9, 1998

REFERENCES

Abou Elela S, Ares MJ. 1998. Depletion of yeast RNase III blocks correct U2 3′ end formation and results in polyadenylated but functional U2 snRNA. *EMBO J 17*:3737–3746.

Amiri KA. 1994. Fibrillarin-like proteins occur in the domain of *Archaea*. *J Bacteriol 176*:2124–2127.

Bachellerie J-P, Michot B, Nicoloso M, Balakin A, Ni J, Fournier MJ. 1995. Antisense snoRNAs: A family of nucleolar RNAs with long complementarities to rRNA. *Trends Biochem Sci 20*:261–264.

Balakin AG, Smith L, Fournier MJ. 1996. The RNA world of the nucleolus: Two major families of small RNAs defined by different box elements with related functions. *Cell 85*:823–834.

Baserga SJ, Yang XW, Steitz JA. 1991. An intact Box C in the U3 snoRNA is required for binding of fibrillarin, the protein common to the major family of nucleolar snRNPs. *EMBO J 10*:2645–2651.

Beltrame M, Henry Y, Tollervey D. 1994. Mutational analysis of an essential binding site for the U3 snoRNA in the 5′ external transcribed spacer of yeast pre-rRNA. *Nucleic Acids Res 22*:4057–4065.

Beltrame M, Tollervey D. 1992. Identification and functional analysis of two U3 binding sites on yeast pre-ribosomal RNA. *EMBO J 11*:1531–1542.

Beltrame M, Tollervey D. 1995. Base-pairing between U3 and the pre-ribosomal RNA is required for 18S rRNA synthesis. *EMBO J 14*:4350–4356.

Bonneaud N, Ozier-Kalogeropoulos O, Li G, Labouesse M, Minvielle-Sebastia L, Lacroute F. 1991. A family of low and high copy replicative, integrative and single-stranded *S. cerevisiae/E. coli* shuttle vectors. *Yeast 7*:609–615.

Bult CJ, White O, Olsen GJ, Zhou L, Fleischmann RD, Sutton GG, Blake JA, FitzGerald LM, Clayton RA, Gocayne JD, Kerlavage AR, Dougherty BA, Tomb JF, Adams MD, Reich CI, Overbeek R, Kirkness EF, Weinstock KG, Merrick JM, Glodek A, Scott JL, Geoghagen NSM, Venter JC. 1996. Complete genome sequence of the methanogenic archaeon, *Methanococcus jannaschii*. *Science 273*:1058–1073.

Caffarelli E, De Gregorio E, Fatica A, Prislei S, Fragapane P, Bozzoni I. 1996. Processing of the intron-encoded U16 and U18 snoRNAs: The conserved C and D boxes control both the processing reactions and the stability of the mature snoRNAs. *EMBO J 15*:1121–1131.

Caffarelli E, Losito M, Giorgi C, Fatica A, Bozzoni I. 1998. In vivo identification of nuclear factors interacting with the conserved elements of box C/D small nucleolar RNAs. *Mol Cel Biol 18*:1023–1028.

Cavaillé J, Bachellerie JP. 1996. Processing of fibrillarin-associated snoRNAs from pre-mRNA introns: An exonucleolytic process exclusively directed by the common stem-box terminal structure. *Biochimie 78*:443–456.

Cavaillé J, Nicoloso M, Bachellerie J-P. 1996. Targeted ribose methylation of RNA in vivo directed by tailored antisense RNA guides. *Nature 383*:732–735.

Cecconi F, Mariottini P, Amaldi F. 1995. The *Xenopus* intron-encoded U17 snoRNA is produced by exonucleolytic processing of its precursor in oocytes. *Nucleic Acids Res 23*:4670–4676.

Chamberlain JR, Lee Y, Lane WS, Engelke DR. 1998. Purification and characterization of the nuclear RNase P holoenzyme complex reveals extensive subunit overlap with RNase MRP. *Genes & Dev 12*:1678–1690.

Chanfreau G, Rotondo G, Legrain P, Jacquier A. 1997. Processing of a dicistronic small nucleolar RNA precursor by the RNA endonuclease Rnt1. *Genes & Dev 11*:2741–2751.

Chu S, Zengel JM, Lindhal L. 1997. A novel protein shared by RNase MRP and RNase P. *RNA 3*:382–391.

Dichtl B, Tollervey D. 1997. Pop3p is essential for the activity of the RNase MRP and RNase P ribonucleoproteins. *EMBO J 16*:417–429.

Eichler DC, Craig N. 1994. Processing of eukaryotic ribosomal RNA. *Prog Nucleic Acids Res Mol Biol 49*:197–239.

Forster AC, Altman S. 1990. Similar cage-shaped structures for the RNA components of all ribonuclease P and ribonuclease MRP enzymes. *Cell 62*:407–409.

Fournier MJ, Maxwell ES. 1993. The nucleolar snRNAs: Catching up with the spliceosomal snRNAs. *Trends Biol Sci 18*:131–135.

Ganot P, Bortolin M-L, Kiss T. 1997a. Site-specific pseudouridine formation in preribosomal RNA is guided by small nucleolar RNAs. *Cell 89*:799–809.

Ganot P, Caizergues-Ferrer M, Kiss T. 1997b. The family of box ACA small nucleolar RNAs is defined by an evolutionarily defined secondary structure and ubiquitous sequence elements essential for RNA accumulation. *Genes & Dev 11*:941–956.

Gautier T, Bergès T, Tollervey D, Hurt EC. 1997. Nucleolar KKE/D repeat proteins Nop56p and Nop58p interact with Nop1p and are required for ribosome biogenesis. *Mol Cell Biol 17*:7088–7098.

Girard JP, Lehtonen H, Caizergues-Ferrer M, Amalric F, Tollervey D, Lapeyre B. 1992. GAR1 is an essential small nucleolar RNP protein required for pre-rRNA processing in yeast. *EMBO J 11*:673–682.

Goodall GJ, Wiebauer K, Filipowicz W. 1990. Analysis of pre-mRNA processing in transfected plant protoplasts. *Methods Enzymol 181*:148–161.

Heiss NS, Knight SW, Vulliamy TJ, Klauck SM, Wiemann S, Mason PJ, Poustka A, Dokal I. 1998. X-linked dyskeratosis congenita is caused by mutations in a highly conserved gene with putative nucleolar functions. *Nat Genet 19*:32–38.

Henras A, Henry Y, Bousquet-Antonelli C, Noaillac-Depeyre J, Gélugne JP, Caizergues-Ferrer M. 1998. Nhp2p and Nop10p are essential for the function of H/ACA snoRNPs. *EMBO J 17*:7078–7090.

Henriquez R, Blobel G, Aris JP. 1990. Isolation and sequencing of NOP1. A yeast gene encoding a nucleolar protein homologous to a human autoimmune antigen. *J Biol Chem 265*:2209–2215.

Hernandez-Verdun D. 1991. The nucleolus today. *J Cell Sci 99*:465–471.

Huang GH, Jarmolowski A, Struck JCR, Fournier MF. 1992. Accumulation of U14 small nuclear RNA in *Saccharomyces cerevisiae* requires box C, box D, and a 5′,3′ terminal stem. *Mol Cell Biol 12*:4456–4463.

Hughes JMX, Ares MJ. 1991. Depletion of U3 small nucleolar RNA inhibits cleavage in the 5′ external transcribed spacer of yeast pre-ribosomal RNA and impairs formation of 18S ribosomal RNA. *EMBO J 10*:4231–4239.

Kiss T, Bortolini M-L, Filipowicz W. 1996. Characterization of the intron-encoded U19 RNA, a new mammalian small nucleolar RNA that is not associated with fibrillarin. *Mol Cell Biol 16*:1391–1400.

Kiss T, Filipowicz W. 1995. Exonucleolytic processing of small nucleolar RNAs from pre-mRNA introns. *Genes & Dev 9*:1411–1424.

Kiss-László Z, Henry Y, Bachellerie J-P, Caizergues-Ferrer M, Kiss T. 1996. Site-specific ribose methylation of pre ribosomal RNA: A novel function for small nucleolar RNAs. *Cell 85*:1077–1088.

Kiss-László Z, Henry Y, Kiss T. 1998. Sequence and structural elements of methylation guide snoRNAs essential for site-specific ribose methylation of pre-rRNA. *EMBO J 17*:797–807.

Klenk HP, Clayton RA, Tomb JF, White O, Nelson KE, Ketchum KA, Dodson RJ, Gwinn M, Hickey EK, Peterson JD, Richardson DL, Kerlavage AR, Graham DE, Kyrpides NC, Fleischmann RD, Quackenbush J, Lee NH, Sutton GG, Gill S, Kirkness EF, Dougherty BA, McKenney K, Adams MD, Loftus B, Venter JC, et al. 1997. The complete genome sequence of the hyperthermophilic, sulphate-reducing archaeon *Archaeoglobus fulgidus*. *Nature 390*:364–370.

Koonin EV. 1996. Pseudouridine synthases: Four families of enzymes containing a putative uridine-binding motif also conserved in dUTPases and dCTP deaminases. *Nucleic Acids Res 24*:2411–2415.

Lafontaine D, Tollervey D. 1995. *Trans*-acting factors in yeast pre-rRNA and pre-snoRNA processing. *Biochem Cell Biol 73*:803–812.

Lafontaine D, Tollervey D. 1996. One-step PCR mediated strategy for the construction of conditionally expressed and epitope tagged yeast proteins. *Nucleic Acids Res 24*:3469–3472.

Lafontaine D, Vandenhaute J, Tollervey D. 1995. The 18S rRNA dimethylase Dim1p is required for pre-ribosomal RNA processing in yeast. *Genes & Dev 9*:2470–2481.

Lafontaine DLJ, Bousquet-Antonelli C, Henry Y, Caizergues-Ferrer M, Tollervey D. 1998a. The box H+ACA snoRNAs carry Cbf5p, the putative rRNA pseudouridine synthase. *Genes & Dev 12*:527–537.

Lafontaine DLJ, Preiss T, Tollervey D. 1998b. Yeast 18S rRNA dimethylase Dim1p: A quality control mechanism in ribosome synthesis? *Mol Cell Biol 18*:2360–2370.

Lafontaine DLJ, Tollervey D. 1998. Birth of the snoRNPs: The evolution of the modification-guide snoRNAs. *Trends Biol Sci 23*:383–388.

Lange TS, Borovjagin A, Maxwell ES, Gerbi SA. 1998a. Conserved boxes C and D are essential nucleolar localization elements of U14 and U18 snoRNAs. *EMBO J 17*:3176–3187.

Lange TS, Borovjagin AV, Gerbi SA. 1998b. Nucleolar localization elements in U8 snoRNA differ from sequences required for rRNA processing. *RNA 4*:789–800.

Lange TS, Ezrokhi M, Borovjagin AV, Rivera-Leon R, North MT, Gerbi SA. 1998c. Nucleolar localization elements of *Xenopus laevis* U3 small nucleolar RNA. *Mol Biol Cell 9*:2973–2985.

Lapeyre B, Mariottini P, Mathieu C, Ferrer P, Amaldi F, Amalric F, Cazergues-Ferrer M. 1990. Molecular cloning of *Xenopus* fibrillarin, a conserved U3 small nucleolar ribonucleoprotein recognized by antisera from humans with autoimmune disease. *Mol Cell Biol 10*:430–434.

Li HV, Zagorski J, Fournier MJ. 1990. Depletion of U14 small nuclear RNA (snR128) disrupts production of 18S rRNA in *Saccharomyces cerevisiae*. *Mol Cell Biol 10*:1145–1152.

Liang W-Q, Fournier MJ. 1995. U14 base-pairs with 18S rRNA: A novel snoRNA interaction required for rRNA processing. *Genes & Dev 9*:2433–2443.

Lygerou Z, Mitchell P, Petfalski E, Séraphin B, Tollervey D. 1994. The *POP1* gene encodes a protein component common to the RNase MRP and RNase P ribonucleoproteins. *Genes & Dev 8*:1423–1433.

Maden BEH. 1990. The numerous modified nucleotides in eukaryotic ribosomal RNA. *Prog Nucleic Acids Res Mol Biol 39*:241–303.

Maden BEH, Hughes JMX. 1997. Eukaryotic ribosomal RNA: The recent excitement in the nucleotide modification problem. *Chromosoma 105*:391–400.

Madore SJ, Wieben ED, Kunkel GR, Pederson T. 1984a. Precursors of U4 small nuclear RNA. *J Cell Biol 99*:1140–1144.

Madore SJ, Wieben ED, Pederson T. 1984b. Intracellular site of U1 small nuclear RNA processing and ribonucleoprotein assembly. *J Cell Biol 98*:188–192.

Maxwell ES, Fournier MJ. 1995. The small nucleolar RNAs. *Ann Rev Biochem 35*:897–934.

Mélèse T, Xue Z. 1995. The nucleolus: An organelle formed by the act of building a ribosome. *Curr Opin Cell Biol 7*:319–324.

Morrissey JP, Tollervey D. 1993. Yeast snR30 is a small nucleolar RNA required for 18S rRNA synthesis. *Mol Cell Biol 13*:2469–2477.

Morrissey JP, Tollervey D. 1995. Birth of the snoRNPs: The evolution of RNase MRP and the eukaryotic pre-rRNA processing system. *Trends Biol Sci 20*:78–82.

Ni J, Tien AL, Fournier MJ. 1997. Small nucleolar RNAs direct site-specific synthesis of pseudouridine in ribosomal RNA. *Cell 89*:565–573.

Nicoloso M, Qu L-H, Michot B, Bachellerie J-P. 1996. Intron-encoded, antisense small nucleolar RNAs: The characterization of nine novel species points to their direct role as guides for the 2′-*O*-ribose methylation of rRNAs. *J Mol Biol 260*:178–195.

Ochs RL, Lischwe MA, Spohn WH, Busch H. 1985. Fibrillarin: A new protein of the nucleolus identified by autoimmune sera. *Biol Cell 54*:123–133.

Ooi SL, Samarsky DA, Fournier MJ, Boeke JD. 1998. Intronic snoRNA biosynthesis in *Saccharomyces cerevisiae* depends on the lariat-debranching enzyme: Intron length effects and activity of a precursor snoRNA. *RNA 4*:1096–1110.

Petfalski E, Dandekar T, Henry Y, Tollervey D. 1998. Processing of the precursors to small nucleolar RNAs and rRNAs requires common components. *Mol Cell Biol 18*:1181–1189.

Qu L-H, Henry Y, Nicoloso M, Michot B, Azum M-C, Renalier M-H, Caizergues-Ferrer M, Bachellerie J-P. 1995. U24, a novel intron-incoded small nucleolar RNA with two 12 nt long, phylogenetically conserved complementarities to 28S rRNA. *Nucleic Acids Res 23*:2669–2676.

Raué HA, Planta RJ. 1991. Ribosome biogenesis in yeast. *Prog Nucleic Acids Res Mol Biol 41*:89–129.

Reeder RH. 1990. rRNA synthesis in the nucleolus. *Trends Genet 6*:390–395.

Samarsky DA, Fournier MJ, Singer RH, Bertrand E. 1998. The snoRNA box C/D motif directs nucleolar targeting and also couples snoRNA synthesis and localization. *EMBO J 17*:3747–3757.

Schimmang T, Tollervey D, Kern H, Frank R, Hurt EC. 1989. A yeast nucleolar protein related to mammalian fibrillarin is associated with small nucleolar RNA and is essential for viability. *EMBO J 8*:4015–4024.

Séraphin B, Rosbash M. 1989. Identification of functional U1 snRNA-pre-mRNA complexes committed to spliceosome assembly and splicing. *Cell 59*:349–358.

Smith DR, Doucette-Stamm LA, Deloughery C, Lee H, Dubois J, Aldredge T, Bashirzadeh R, Blakely D, Cook R, Gilbert K, Harrison D, Hoang L, Keagle P, Lumm W, Pothier B, Qiu D, Spadafora R, Vicaire R, Wang Y, Wierzbowski J, Gibson R, Jiwani N, Caruso A, Bush D, Reeve JN, et al. 1997. Complete genome sequence of *Methanobacterium thermoautotrophicum* deltaH: Functional analysis and comparative genomics. *J Bacteriol 179*:7135–7155.

Sollner-Webb B, Tycowski KT, Steitz JA. 1996. Ribosomal RNA processing in eukaryotes. In: *Ribosomal RNA: Structure, evolution, processing, and function in protein biosynthesis*. pp 469–490.

Tollervey D. 1996. *Trans*-acting factors in ribosome synthesis. *Exp Cell Res 229*:226–232.

Tollervey D, Kiss T. 1997. Function and synthesis of small nucleolar RNAs. *Curr Opin Cell Biol 9*:337–342.

Tollervey D, Lehtonen H, Carmo-Fonseca M, Hurt EC. 1991. The small nucleolar RNP protein NOP1 (fibrillarin) is required for pre-rRNA processing in yeast. *EMBO J 10*:573–583.

Tollervey D, Lehtonen H, Jansen R, Kern H, Hurt EC. 1993. Temperature-sensitive mutations demonstrate roles for yeast fibrillarin in pre-rRNA processing, pre-rRNA methylation, and ribosome assembly. *Cell 72*:443–457.

Venema J, Tollervey D. 1995. Processing of pre-ribosomal RNA in *Saccharomyces cerevisiae*. *Yeast 11*:1629–1650.

Warner JR. 1989. Synthesis of ribosomes in *Saccharomyces cerevisae*. *Microbiol Rev 53*:256–271.

Watkins NJ, Gottschalk A, Neubauer G, Kastner B, Fabrizio P, Mann M, Lührmann R. 1998a. Cbf5p, a potential pseudouridine synthase, and Nhp2p, a putative RNA-binding protein, are present together with Gar1p in all H box/ACA-motif snoRNPs and constitute a common bipartite structure. *RNA 4*:1549–1568.

Watkins NJ, Leverette RD, Xia L, Andrews MT, Maxwell ES. 1996. Elements essential for processing intronic U14 snoRNA are located at the termini of the mature snoRNA sequence and include conserved nucleotide boxes C and D. *RNA 2*:118–133.

Watkins NJ, Newman DR, Kuhn JF, Maxwell ES. 1998b. In vitro assembly of the mouse U14 snoRNP core complex and identification of a 65-kDa box C/D-binding protein. *RNA 4*:582–593.

Weaver P, Sun C, Chang T-H. 1997. Dpb3p, a putative RNA helicase in *Saccharomyces cerevisiae*, is required for efficient pre-rRNA processing predominantly at site A_3. *Mol Cell Biol 17*:1354–1365.

Wu P, Brockenbrough JS, Metcalfe AC, Chen S, Aris JP. 1998. Nop5p is a small nucleolar ribonucleoprotein component required for pre-18 S rRNA processing in yeast. *J Biol Chem 273*:16453–16463.

Xia L, Watkins NJ, Maxwell ES. 1997. Identification of specific nucleotide sequences and structural elements required for intronic U14 snoRNA processing. *RNA 3*:17–26.

Yuo CY, Ares M Jr, Weiner AM. 1985. Sequences required for 3′ end formation of human U2 small nuclear RNA. *Cell 42*:193–202.